Kent Academic Repository
Full text document (pdf)

Citation for published version

DOI

Link to record in KAR

https://kar.kent.ac.uk/78035/

Document Version

Publisher pdf

Mucoadhesion of Progesterone-Loaded Drug Delivery Nanofiber Constructs

Francis Brako,[†,‡] Richard Thorogate,[§] Suntharavathanan Mahalingam,[†] Bahijja Raimi-Abraham,[‡,∥] Duncan Q. M. Craig,[‡] and Mohan Edirisinghe*[†]

[†]Department of Mechanical Engineering, University College London, Torrington Place, London WC1E 7JE, U.K.
[‡]School of Pharmacy, University College London, 29-39 Brunswick Square, London WC1N 1AX, U.K.
[§]London Nanotechnology Centre, 19 Gordon Street, Bloomsbury, London WC1H 0AH, U.K.

ABSTRACT: Mucoadhesive delivery systems have attracted remarkable interest recently, especially for their potential to prolong dosage form resident times at sites of application such as the vagina or nasal cavity, thereby improving convenience and compliance as a result of less frequent dosage. Mucoadhesive capabilities need to be routinely quantified during the development of these systems. This is however logistically challenging due to difficulties in obtaining and preparing viable mucosa tissues for experiments. Utilizing artificial membranes as a suitable alternative for quicker and easier analyses of mucoadhesion of these systems is currently being explored. In this study, the mucoadhesive interactions between progesterone-loaded fibers (with varying carboxymethyl cellulose (CMC) content) and either artificial (cellulose acetate) or mucosa membranes are investigated by texture analysis and results across models are compared. Mucoadhesion to artificial membrane was about 10 times that of mucosa, though statistically significant ($p = 0.027$) association between the 2 data sets was observed. Furthermore, a hypothesis relating fiber−mucosa interfacial roughness (and unfilled void spaces on mucosa) to mucoadhesion, deduced from some classical mucoadhesion theories, was tested to determine its validity. Points of interaction between the fiber and mucosa membrane were examined using atomic force microscopy (AFM) to determine the depths of interpenetration and unfilled voids/roughness, features crucial to mucoadhesion according to the diffusion and mechanical theories of mucoadhesion. A Kendall's tau and Goodman−Kruskal's gamma tests established a monotonic relationship between detaching forces and roughness, significant with p-values of 0.014 and 0.027, respectively. A similar relationship between CMC concentration and interfacial roughness was also confirmed. We conclude that AFM analysis of surface geometry following mucoadhesion can be explored for quantifying mucoadhesion as data from interfacial images correlates significantly with corresponding detaching forces, a well-established function of mucoadhesion.

KEYWORDS: mucoadhesion, interpenetration, interface, nanofiber, mucin
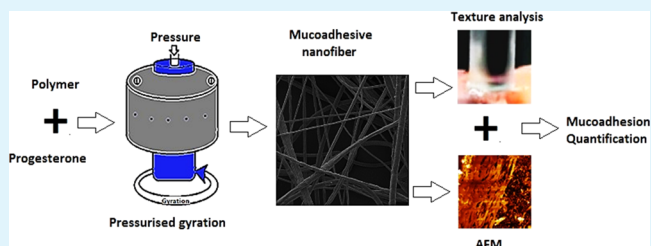
1. INTRODUCTION

Mucoadhesion is defined as an interactive state in which two material surfaces, at least one being biological in nature and typically a mucosa membrane, are held together by interfacial forces for a prolonged period of time.[1] Utilizing mucoadhesion for more effective drug delivery has and continues to attract more attention within the pharmaceutical sciences, as substantial evidence exists to support claims of improved dosage form residence time, therapeutic efficacy, improved drug targeting in cancer therapy, and delivery of biologicals such us peptides and antibodies through a variety of routes of administration such as ocular, nasal, buccal, and vaginal.[2,3]

Nanofibers, described as slender, elongated thread-like structures within the nanoscale range, are emerging strongly as the material of choice for drug delivery. Due to their large surface area, unique surface topology, porosity, and minimal moisture content, nanofibers are known to significantly improve the adhesiveness of the systems utilizing them.[4,5] Furthermore, their ability to enhance drug solubility and high

adsorption efficiency potentially make them suitable carriers for transmucosal drug delivery.[4] Producing substantial quantities of nanofibers with good mucoadhesive prospects will be a positive addition to efforts in improving drug delivery across mucosa membranes.

The exact mechanism underlying mucoadhesion remains under discussion.[6] Notwithstanding, classical observational theories explain mucoadhesion in two main steps, regardless of the underlying theory. These are the contact stage and the consolidation stage.[7,8] The first step involves the spreading and swelling of the mucoadhesive material to facilitate extensive contact with the mucosal membrane. At the consolidation stage, the mucoadhesive materials interact with the membrane; one suggestion being that moisture plasticizes the systems allowing molecules from these materials to break free and form

Table 1. Composition and Properties of Solutions Used in Generating Progesterone-Loaded Fibers

sample	solution composition			solution properties	
	progesterone (wt %)	PEO (wt %)	CMC (wt %)	viscosity (mPa/s) ± SD	surface tension (mN/m) ± SD
A	5	15.00	0	7593 ± 13	55.7 ± 0.4
B	5	14.25	0.75	7719 ± 21	56.1 ± 0.7
C	5	13.75	1.25	8220 ± 30	56.7 ± 0.4
D	5	13.25	1.75	8617 ± 27	57.5 ± 0.2
E	5	12.50	2.50	9033 ± 39	58.3 ± 0.7

linkages with mucins in the mucosal layer by weak van der Waals and hydrogen bonds.[1] Both contact and consolidation stages work together to bring about mucoadhesion.

In addition to the two-step principle of mucoadhesion, several theories have been used to explain this complex phenomenon. These include the electrostatic explanation, where opposing electrical charges from the interacting surfaces sustain mucoadhesion. Others are the adsorption theory, which suggests that a mucoadhesive device is held to the mucosa surface by secondary chemical interactions such as hydrogen bonding and electrostatic attraction, whereas the wetting theory describes the affinity between the surfaces facilitated by surface energetics, predominantly in liquid bioadhesive systems.[9,10] On the other hand, the diffusion theory, which is used quite extensively, explains how mucoadhesion is brought about by interpenetration of polymer and mucin chains into each other. The rate and extent of penetration, dependent on such factors as diffusion coefficient and nature of mucoadhesive chains, their mobility, and contact time, determine the strength of mucoadhesion.[11] The fracture theory, presently used widely in studying mucoadhesion, explains mucoadhesion in terms of the amount of force required to completely detach the interacting surfaces.[12,13] Last of all, there is the mechanical theory that describes mucoadhesion in terms of surface roughness and the filling up of irregular surface spaces, interfacial surface behavior, and surface energy dissipation.[14]

Quantifying mucoadhesion remains challenging and is the subject of several investigations.[11,15] Several methods, including measuring forces required to detach interacting surfaces,[6] tracking the extent of polymer reaction with mucin, for instance by measuring fluorescence intensities, ζ-potential, or levels of turbidity,[16,17] and more recently, by using atomic force microscopy (AFM) to study footprints, such us dried out surfaces prior to mucoadhesion,[18−20] have been attempted for quantifying mucoadhesion. Bond energies involved in polymer−mucin interactions can cause macromolecular rearrangements exhibited as changes in viscosity.[6] Rheological methods, based on analyzing these viscosity changes, are also commonly used in quantifying mucoadhesion.

The pressurized gyration (PG) approach to producing fibers of various sizes and shapes from a wide range of materials, following reports of several studies,[20−24] is proving to be a suitable alternative to electrospinning. The simplicity, versatility, and especially flexibility with choice of materials make this an ideal method of making nano- and microfibers. Restrictions with solvent choice limit the usefulness of electrospinning in generating materials for pharmaceutical applications. PG has no such requirement and therefore suitable for generating nano- and microfibers from a wider range of materials. PG is fundamentally driven by the principles of Rayleigh−Taylor instability and Marangoni effect,[22,25] where high rotational forces on system of fluids with different densities (basically polymer solution and air) creates the necessary fluid

acceleration and instability at the interface that eventually cause a breakaway in the form of jets. These jets are further stretched due to sustained stress from the forces, primarily centrifugal and gravitational, acting on the system. Evaporation of solvent during flight of jet from vessel through the nozzle ensures thinning and completes the fiber formation process.

In this study, as well as producing and characterizing progesterone-loaded fibers by PG, the relationship between interfacial roughness (following interaction between progesterone-loaded fiber and mucosa) and mucoadhesion is investigated using AFM. According to the mechanical and diffusion theories, adequate filling up of cavities on mucosa surface and more extensive interpenetration of polymer and mucin functional groups should result in stronger mucoadhesion. Extent of polymer−mucin interpenetration and filling up voids on mucosa surface should leave a commensurate interfacial roughness following mucoadhesion. It was therefore hypothesized that a nanoscale analyses of these surfaces by a suitable method like AFM could offer trends useful for quantifying mucoadhesion. Testing this hypothesis is the basis for this study. Fracture properties and interfacial roughness of the two surfaces in mucoadhesive interaction were studied using texture analyzer and AFM respectively. Data from these two sets of experiments were statistically examined to determine significant correlations. As the study sought to investigate the strength of associations between data sets from either different mucoadhesion models or methods of quantification, Kendall's tau and/or Goodman−Kruskal's gamma analyses were used in testing the hypotheses being determined.

This fiber mucoadhesion investigations are crucial part of a project seeking to develop novel fiber-based vaginal dosage forms, where mucoadhesive fibers from various polymer blends have been developed[20] and suitable candidates selected and loaded with progesterone, performing as functional drug delivery systems.[26]

2. EXPERIMENTAL DETAILS

2.1. Materials. Sodium carboxymethylcellulose (CMC) ($M_w \sim$ 250 000 g/mol), poly(ethylene oxide) (PEO) ($M_w \sim$ 200 000 g/mol), progesterone ($M_w \sim$ 314 g/mol, aqueous solubility: 8.81 mg/L (at 25 °C), log P: 3.87), and ethanol (analytical grade) were obtained from Sigma-Aldrich, Gillingham, U.K. All were used without further purification. Purified water and their mixtures with ethanol were used as solvents throughout the study. Simulated vaginal fluid (SVF) was prepared according to the formula developed by Owen and Katz (1999)[27] and contained sodium chloride (3.51 g/L), potassium hydroxide (1.40 g/L), calcium hydroxide (0.222 g/L), and bovine serum albumin (0.018 g/L). The remaining ingredients were acetic acid (1.00 g/L), lactic acid (2.00 g/L), glucose (5.0 g/L), urea (0.4 g/L), glycerol (0.16 g/L), and porcine mucin type II (1.5% w/v). All of these were also obtained from Sigma-Aldrich. Cellulose acetate of pore size 0.2 μm, used as artificial membrane in mucoadhesive studies, was obtained from Sartorius, Gottingen, Germany. Fresh mucosa for

mucoadhesive study was from lamb esophageal tissue arranged and delivered by Giggly Pigs, Romford, U.K.

2.2. Methods. *2.2.1. Solution Preparation and Characterization.* Uniform drug−polymer solutions of progesterone and PEO or PEO/ CMC were obtained by continuous magnetic stirring followed by sonication for 10 min using a Branson Sonifier 250 (Danbury, CT). The viscosity of each polymer solution or blend was measured using a Brookfield DV-111 viscometer (Harlow, Essex, U.K.) at a shear stress of 3.5 Pa. Water running through a jacket surrounding the column containing solutions ensured a constant temperature of 22 °C throughout the measurements. The surface tension was measured by the Wilhelmy plate method using a Kruss K9 tensiometer (Hamburg, Germany), also at an ambient temperature of 22 °C. For each solution, five separate calibrated measurements for viscosity and surface tension were taken and their means used for further analyses. Solution constituents and their properties are shown in Table 1.

2.2.2. Fiber Formation. To make progesterone-loaded fibers, 3 mL of solution was placed in the aluminum vessel and spun at a rotational speed of 24 000 rpm and working pressure of 0.15 MPa. The combined pressure and centrifugal force cause an ejection of fluid in very fine streams through the orifices. The solvent is then evaporated off the jet during flight, leaving a fibrous material on the surrounding collecting shields. Each manufacturing cycle takes approximately 3 min and fibers produced were collected and stored until required for further analyses. Fibers were successfully spun from solutions with up to 2.5 wt % of CMC, beyond which it was not possible to generate well-structured fibers.

2.2.3. Scanning Electron Microscope (SEM) Imaging and Size Distribution Analysis. Samples from each batch of fibers were analyzed by scanning electron microscope (SEM), JEOL JSM 630 IF (Tokyo, Japan) for the morphology, and in particular the size distribution of fibers. Fibers were mounted on SEM stubs with the aid of two-sided adhesive carbon disks obtained from Agar Scientific, Stansted, U.K. Each mounted sample of fibers was gold coated for 90 s using Quorum Q150R pumped sputter coaters (Quorum Technologies, Lewes, U.K.). Coated samples were analyzed at an operating voltage of 5 kV. The record of images was produced with the aid of SemAfore software, also provided by the SEM manufacturer. The average fiber diameter and size distribution for each batch was determined from measurements of least 100 fiber diameters using ImageJ software (National Institute of Health, MD).

2.2.4. Mucoadhesion. The extent of interactions between nanofibers and mucosa membrane surface were studied using a Texture analyzer, TA-XT2 (Stable Micro Systems Ltd., Surrey, U.K.) under the experimental conditions shown in Table 2. The mucosa membrane from lamb esophageal tissue, known to be non-keratinized and similar to human esophageal mucosa[28] in dimensions of 40 × 30 mm² was firmly attached onto the stage of the texture analyzer with the help of adhesive tapes.

Samples of nanofibers (100 mg) whose mucoadhesive potential is being assessed were securely attached to a cylindrical probe (Chen−Hoseney dough stickiness rig) with a cross-sectional area of 0.785 cm²

Table 2. Experimental Condition Selected for Measuring Forces Required to Detach Fibers from Mucosa

velocity	
pretest	50 mm/s
test	50 mm/s
post-test	10 mm/s
tracking	5 mm/s
force	
test force	20 gF
trigger force	10 gF
distance	
return distance	4 mm
time	
contact time	5 s

using double-sided adhesive disks. This was mounted on the movable part of the analyzer. The analyzer was set to measure the force required to completely detach the nanofiber from the mucosa membrane after bringing the two materials together for a contact time of 5 second with a pretest force of 20 gF (0.2 N). This routine was conducted in triplicates for all the samples and the means and standard deviations (SD) calculated for further analyses. The same procedure was repeated using 0.2 μm pore-sized cellulose acetate membrane treated with SVF to confer some mucosa properties. Cellulose acetate with this pore dimension was selected for comparison with actual mucosa membrane, as they were confirmed to correlate well with each other when utilized in some permeation studies.[29]

2.2.5. AFM Analyses of Interfaces. Nanofiber (100 mg) was mounted on lamb 12 cm² esophageal mucosa and 0.1 g of SVF (based on the average vaginal surface area of 87 cm² having approximately 0.75 g of fluid at any one time[27,30]) added to facilitate adhesion. SVF (pH = 4.2) was the body fluid selected for this study to maintain an acidic environment, a condition known to potentiate mucoadhesion of anionic polymers such as CMC.[31] The parameter being varied in this work is CMC content in progesterone-loaded fibers and hence crucial to maintain an environment where its impact on mucoadhesion is highlighted. The fiber/mucosa samples were kept at body temperature (37 °C) for 30 min to allow sufficient mucoadhesion, followed by storage at ambient temperature in a desiccator for 48 h to dry out enough to allow sectioning. The transverse sections of the fiber/ mucosa specimen were prepared by cutting with razor blade such that they were thin enough to lie flat with other side exposed for the AFM probes to be brought close to their interface to determine the level of roughness. The dimension icon AFM (Bruker, Coventry, U.K.) with PointProbe Plus Nanosensor probes in tapping mode was employed in measuring the roughness at the interface. The height and phase images and roughness dimensions (R_a and R_{max}) returned from scanning these surfaces were used in further analysis.

3. RESULTS AND DISCUSSION

3.1. Nanofiber Generation, Morphology, and Size Distribution. Nanofibers characterized in this study were generated by PG (Figure 1a), as described in Section 2.2.2. These progesterone-loaded fibrous materials (Figure 1b) are the starting material for the development of vaginal inserts, which will be used to deliver suitable amounts of progesterone for the prevention of premature labor in women considered at high risk. The kinetics of drug release from these progesterone-loaded fibers has been investigated and reported.[26] Mucoadhesive properties of the progesterone-loaded fibers' is also crucial to their performance as drug delivery systems. Therefore as a continuation of our previous work on investigating the release of progesterone from these fiber systems, a range of assessments of mucoadhesion from different perspectives were developed for the purpose of a comprehensive characterization of mucoadhesive prospects of these fibers and reported herein.

These bundle of nanofibers, as seen in Figure 1b, are usually aligned along the vessel circumference during the production because their malleability allows them to be easily molded into any desired shape. Presently, two dosage form options are being considered: a direct compression of nanofibers into tablets[32] for vaginal insertion or winding bundles of the fiber into a miniature tampon.[33]

Crystalline materials including some drugs such as vitamin B6, carbon nanotubes, and metals, when embedded in nanofibers can cause extensive protrusion from within, resulting in an uneven nanofiber surface. Several studies investigating nanofibers containing crystallites have reported this observation.[34−36] The effect of crystalline material content on the
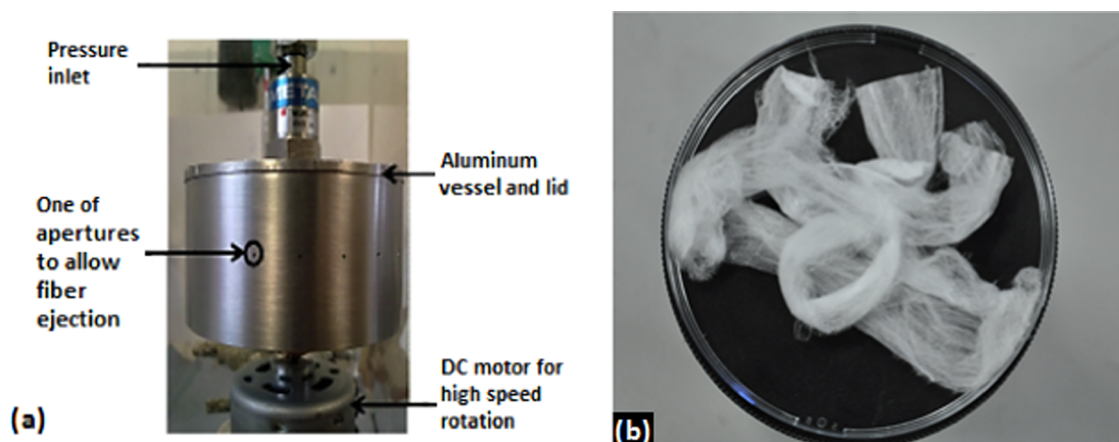
Figure 1. (a) Pressurized gyration apparatus and (b) a bundle of nanofibers generated using (a).
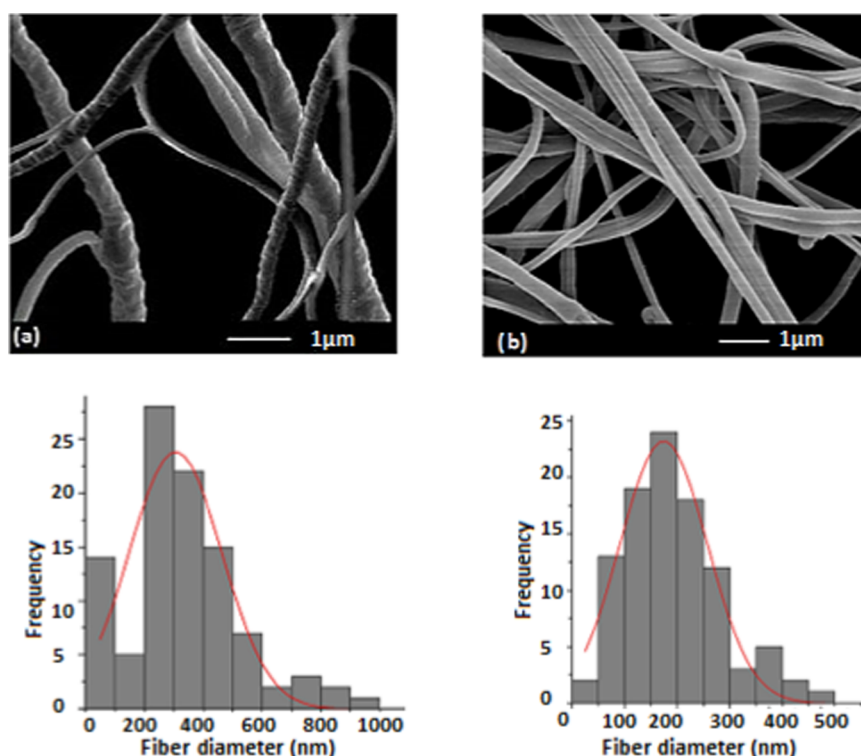

Figure 2. SEM images and size distribution (n = 100) of (a) progesterone-loaded PEO (13.75 wt %)/CMC (1.25 wt %) fiber, average diameter 404 nm with polydispersity index of 0.22 and (b) PEO (13.75 wt %)/CMC (1.25 wt %) fiber without any drug, average diameter 194 nm with polydispersity index of 0.12. The effect of loaded crystalline progesterone in fibers is seen on the surface morphology.

nanofiber surface is particularly relevant in this work as several of the mucoadhesion theories emphasize the relationships between surface properties and their ability to adhere. The necessary adjustments to manage fiber surface disruptions due to crystalline content (both qualitative and quantitative) during formation will be required in order to produce structures with best possible surface properties that support mucoadhesion.

The effects of protrusion by crystalline material in fibers on surface morphology is clearly seen in Figure 2a, drug-loaded nanofiber (approx. 25 wt % of progesterone), especially when compared to nanofibers without any drug (Figure 2b). In terms of dimensions, progesterone loading increased the fiber diameter considerably. This is expected as a 5% loading of progesterone in solutions from which fibers were produced increased viscosity substantially. Whereas a PEO (13.75 wt

%)/CMC (1.25 wt %) solution without progesterone had a viscosity of 5167 mPa s, a 5 wt % loading of progesterone yielded a solution with a viscosity of 8220 mPa s; a change that resulted in more than doubling of the fiber diameter (Figure 2).

A similar trend was seen while varying the CMC content in fibers. It is clear from the plot in Figure 3 that the average diameter of nanofibers was significantly affected by variations in the PEO/CMC ratios. Specifically, the solutions containing higher proportions of CMC yielded fibers with a larger diameter. For instance, increasing the CMC quantities from 1.25 to 2.50 wt % resulted in over 40% increase in the fiber diameter. Whereas a positive correlation between viscosity and fiber outcome in terms of size has been established, surface tension principally correlates to the minimum force required for the initiation of fiber formation, but not necessarily relating to
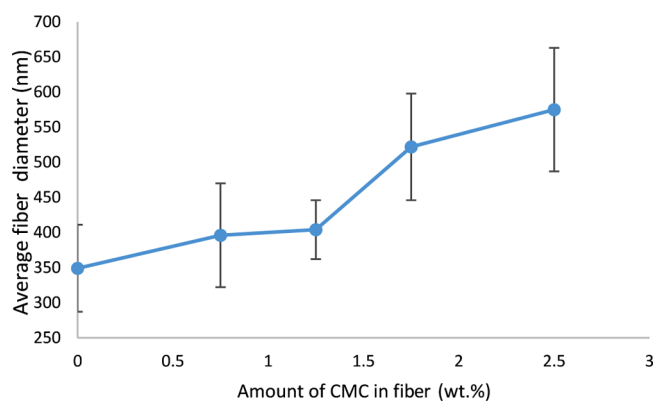
Figure 3. Effect of CMC content on average fiber diameters generated in this work.

Figure 5. Typical trace recorded during attaching and detaching the nanofiber samples from mucosa surfaces. Probe is pressed onto the mucosa and force adjusted until test force of 40 g is attained. Fiber remains in contact with mucosa for 5 s, after which the fiber on the probe tip is separated and force involved measured (detaching force).

its size.[22,37] CMC, primarily incorporated into fibers to influence their mucoadhesion character significantly increased the solution viscosity and subsequently fiber size. This was anticipated to be a likely outcome as CMC is known for its high viscosity in low concentrations,[38] a property also largely dependent on the degree of substitution occurring on the cellulosic backbone and the intrinsic viscosity of plant pulp from which the polymer is derived.[39]

3.2. Mucoadhesive Study. *3.2.1. Artificial versus Natural Membrane.* Two features usually assessed to determine the performance of mucoadhesive delivery systems are (i) their adhesion properties and (ii) the permeation through the mucosa.[40,41] Evaluating both features typically require the use of excised mucosa membranes from animals. The use of animal mucosa tissues, in addition to being costly and logistically challenging, can give rise to inconsistent results due to the widely varying approaches to tissue preparation. To overcome these issues, artificial membranes such as cellulose acetate have been utilized for both adhesive and permeation studies and have been confirmed to correlate well with those obtained from animal mucosa tissues.[29,42]

Mucoadhesive properties of various batches of progesterone-loaded nanofibers were measured using a texture analyzer under test conditions shown in Table 2. A typical trace from stages A−C (Figure 4) encountered during testing is shown graphically in Figure 5. The nanofiber sample attached to the tip of a probe is brought in contact with the membrane surface for 5 s with a test force of 40 gF (0.4 N). The force then required to detach the fiber from the membrane surface is a function of the extent of adhesion occurring between the two surfaces, and is measured and recorded.
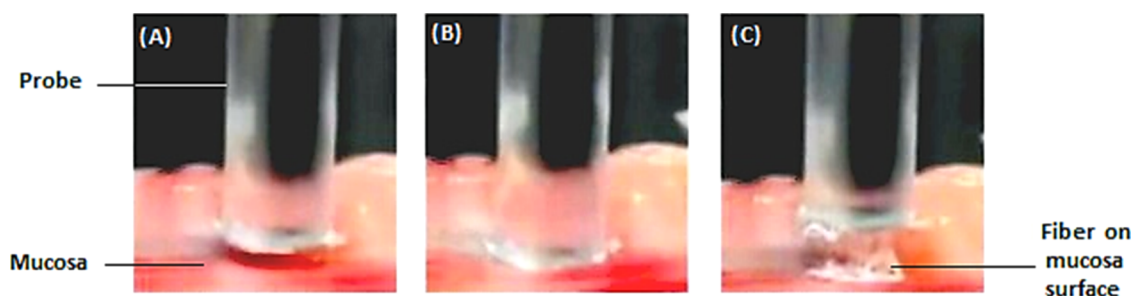
First, the effect of increasing amounts of CMC in fibers on their mucoadhesive properties were studied using both artificial and mucosa membranes. In both instances, a clear trend of increasing mucoadhesive interactions with higher amounts of CMC was established (Figure 6a,b). The stronger mucoadhesion seen with increasing amounts of CMC may be explained using some well-established principles governing the interactions between weakly anionic carboxyl containing polymers with oligosaccharides chains in mucins.[31] The carboxylic groups in these polymers are able to form strong hydrogen bonds with mucin chains, thereby strengthening the interactions between these two materials, leading to appreciable levels of mucoadhesion. The formation of these bonds has been confirmed with the displacement of infrared absorption bands and nuclear magnetic resonance.[43] Furthermore, these weakly anionic polymers demonstrated strongest mucoadhesive interactions in acidic conditions, with adhesive properties diminishing drastically at pH > 4;[44] hence, the experiments were conducted under simulated vaginal conditions (pH = 4.2).

Second, results from fiber mucoadhesive interactions with artificial membrane were compared to those obtained from mucosa. Generally, stronger interactions were observed between the fibers and the artificial membrane than those seen with the lamb mucosa. This observation is expected due to the adhesive behavior of cellulose-based materials mainly driven by the formation of hydrogen bonds by hydroxyl groups present and partially by free energy interactions driven by

Figure 4. Stages in measuring the strength of fiber adhesion to mucosa: (A) analyzer probe with fiber attached to the tip is brought in contact with mucosa membrane, (B) fiber and mucosa are in contact for specified period and (C) fiber is separated from mucosa, whereas force required is measured.
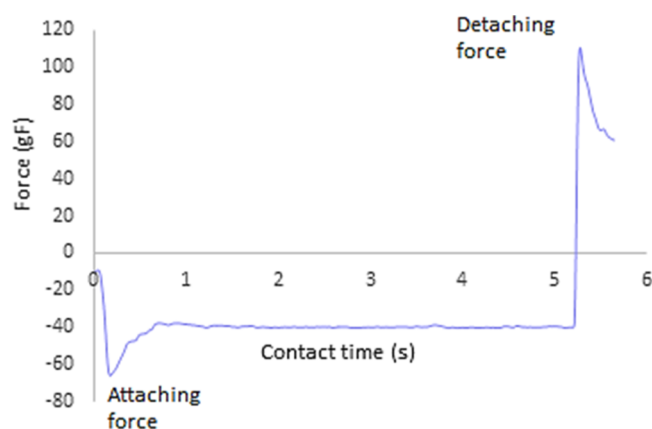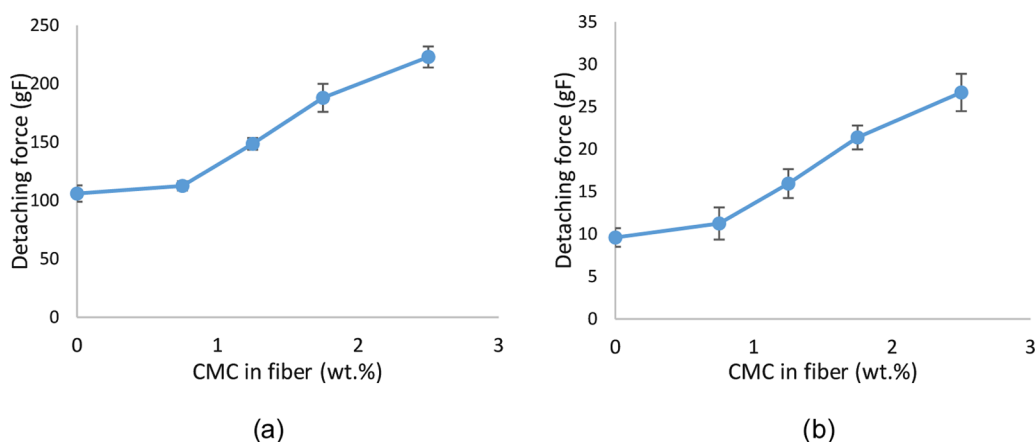
Figure 6. Effect of CMC content on nanofiber mucoadhesive properties assessed by measuring forces required to detach them from (a) cellulose acetate membrane and (b) lamb esophagus mucosa.
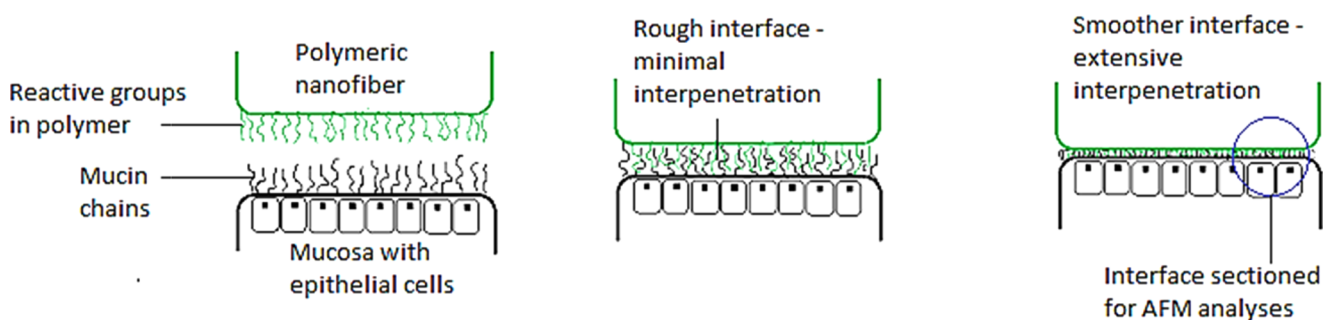

Figure 7. Schematic illustration of interaction between polymer and mucin reactive groups. An extensive interpenetration of groups from two surfaces, according to diffusion theory results in closer (smoother) and stronger adhesion.
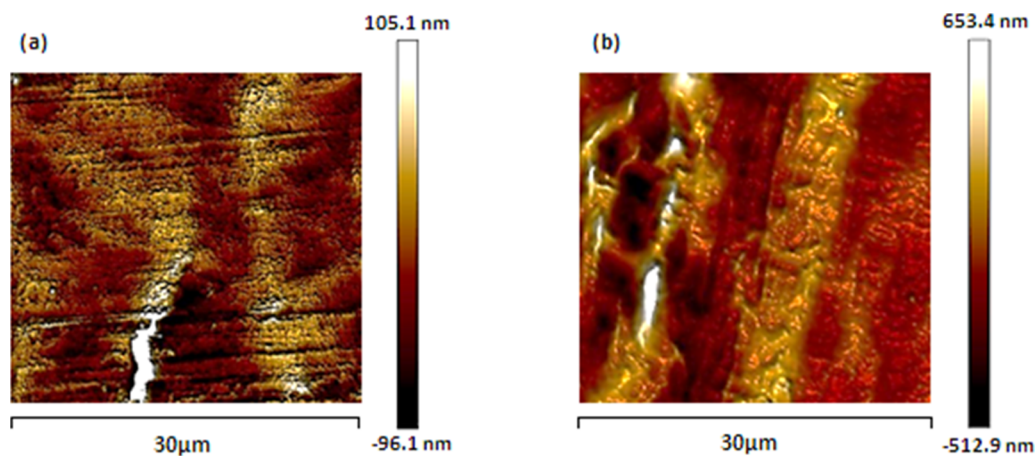

Figure 8. AFM images showing depths (dark regions) and heights (light regions) of sections of interface derived from mucosa membrane interactions with nanofibers (a) containing 2.5% CMC and (b) without CMC. Sections from fibers containing CMC, as seen from scale bar was smoother, indicating closer interactions of surfaces when compared to those from samples without CMC.

apolar and electron donor components of cellulose.[45] Therefore, the higher magnitude of adhesion observed with the cellulose acetate membrane is due to relatively stronger interactions between the fiber and cellulosic components of the membrane. In contrast, the mucoadhesion occurring between the fibers and the lamb mucosa was due to weaker interactions between reactive groups in the fiber and mucin in the mucosa. In terms of trends, a similar correlation between adhesion and CMC content in fibers was observed in both artificial and natural membrane (R^2 = 0.97 and 0.98 as seen in Figure 6a,b). Furthermore, a Kendall's tau test done to determine the strength of correlation between fiber mucoadhesion to artificial and mucosa membranes returned a p-value of 0.027, implying a significant relationship at $p < 0.05$ level. On the basis of these observations, artificial membranes such as cellulose acetate may be suitable for analyzing trends such as those describing changes in mucoadhesion while varying influential parameters. Considering the remarkable difference in magnitude between the progesterone-loaded fiber's adhesion to the cellulose acetate and mucosa membranes, substituting models may not offer reliable outcome, especially when scalar quantification of adhesion is relevant to the study.
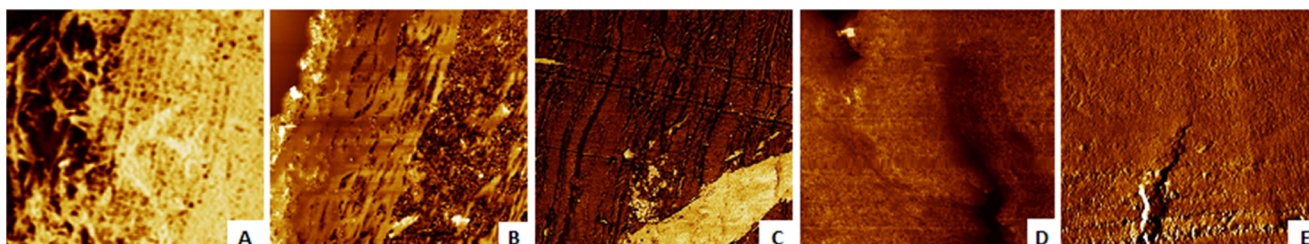
Figure 9. AFM phase images from fiber−mucosa interface following a period of mucoadhesion. Homogeneity (material uniformity) is seen to increase with CMC content in fibers: (A) 0%, (B) 0.75%, (C) 1.25%, (D) 1.75%, (E) 2.5%. Images resized to represent an area of 900 μm^2 with angular units between −30 and 15°.

3.2.2. AFM Analyses of Fiber−Mucosa Interface. In this section, the interface between various batches of progesterone-loaded fibers (shown in Table 1) and mucosa membrane, following mucoadhesive interaction, was visualized by AFM for interfacial roughness. A schematic in Figure 7 illustrates our hypothesis of how interfacial roughness is indicative of interpenetration between surfaces and may correlate with mucoadhesion. Extensive penetration ensures a stronger binding of the surfaces and thus a cross section reveals a smoother (lower height) surface. In the same way, limited interpenetration leaves a rougher surface and that can be taken as minimal mucoadhesion. Whereas the progesterone-loaded fibers studied are intended for vaginal application, the hypothesis set and ensuing investigations are generic for polymer−mucin interactions and not necessarily specific to vaginal mucoadhesion.

The mucosa used in this study, excised from a freshly slaughtered lamb esophagus, was to permit polymer−mucin interactions as would occur in a biological system to a reasonable extent. Further ex vivo experiments with specific mucosa tissues and controls would be required for quantifying mucoadhesion in the particular area of interest.

In comparing the roughness at the interface of various nanofiber samples interactions with mucosa, the parameter routinely used to measure surface roughness was R_a (arithmetic average of absolute height values). R_{max}, which is the total dimension from the lowest depth to the highest point, was also considered, as this is indicative of all unfilled voids (depths) on the mucosa during mucoadhesion.

Interfacial roughness data from fibers with varying CMC concentrations were obtained and tested for possible relationships with mucoadhesive results from texture analyses discussed in Section 3.2.1. Generally, the samples containing higher amount of CMC showed smoother interfacial images. Figure 8 compares the interfacial images following interactions between mucosa and fibers with (a) PEO with 2.5% CMC and (b) PEO only (0% CMC). In the tapping mode, with a phase lag between excitation signal and cantilever response due to difference in material surface interaction with probe tip, the resulting phase imaging is found to go beyond simple topographical mapping to detect variations in composition, adhesion, viscoelasticity, among other properties.[46,47] Phase images from fiber−mucosa interfacial scans are shown in Figure 9A−E. These images reveal increasing level of uniformity as the CMC content in the progesterone-loaded fiber increases from 0% (A) to 2.5% (E).

In addition, roughness data automatically generated from height images by the AFM software and presented in Table 3 showed an inverse correlation with the amount of CMC in the fibers. CMC was anticipated to influence the mucoadhesion of

Table 3. Fiber Composition and Corresponding Interfacial Roughness Measurements Generated from AFM Analysis

fiber	progesterone (wt %)	PEO (wt %)	CMC (wt %)	detaching force (gF)	roughness (nm)	R_{max} (nm)
A	5	15.00	0	9.60	142	1716
B	5	14.25	0.75	11.26	69	610
C	5	13.75	1.25	15.95	37	480
D	5	13.25	1.75	21.39	31	462
E	5	12.5	2.5	26.69	26	439

the progesterone-loaded fibers and hence their inclusion into these systems that are to be used in developing vaginal insert whose performance is aided by mucoadhesion. Indeed, the positive correlation between CMC content and mucoadhesion has been confirmed by texture analyses in Section 3.2.1. The apparent relationship between interfacial roughness data and CMC content confirmed to be a function of mucoadhesion by the well-established texture analysis method offers an opportunity for a quantitative study of mucoadhesion by AFM. A review of the diffusion and mechanical theories that explain mucoadhesion by the degree of molecular interpenetration of groups and filling up of irregular spaces (voids) on the interacting surfaces points to a possibility of studying mucoadhesion by examining the residual surface after adhesion has occurred. Based on these relationships and theories, statistical analyses among detaching forces, roughness (R_a and R_{max}), and CMC concentrations to validate or rule out the hypothesis postulated earlier. It can be concluded that interfacial roughness relates to and can be used to quantify mucoadhesion.

Considering the number of data points and more importantly the need to establish the strength of ordinal associations between the two data sets, Goodman−Kruskal gamma and Kendall's tau tests, two commonly used nonparametric measures for assessing rank correlations, were used. Separate tests were conducted to determine the strength of correlations between detaching force and R_a, detaching force and R_{max}, and finally detaching force and CMC concentration. Goodman−Kruskal gamma and Kendall's tau tests returned p-values of 0.027 and 0.014, respectively (both with statistic of −1 implying an inverse monotonic relationship) for correlations between detaching force and interfacial roughness. Interestingly, the same p-values were obtained from tests between detaching force and CMC concentration, except for a statistic of 1, which indicated a direct monotonic relationship. Similar p-values for all three tests implies similar magnitude of changes occurring in same order when corresponding quantities are varied, an indication of a strong interdependence among the measurements tested. These statistically significant evidence (at $p < 0.05$ level) for monotonic relationships between detaching

forces (determined using texture analyzer) and R_a, R_{max}, and CMC concentration validate the hypothesis of relating interfacial roughness following polymer−mucin interactions to the magnitude of mucoadhesion. The geometry of surfaces (roughness in our case) and indeed many other features such as energetics arising following mucoadhesive interactions, as hinted by the various mucoadhesion theories, offers opportunities for an experimental study of mucoadhesion.

4. CONCLUSIONS

The possibility of generating progesterone-loaded mucoadhesive fibers from a blend of polymers is reported. Loading progesterone into fibers altered the morphology and increased the average fiber diameter. Incorporating CMC into the fibers also increased their mucoadhesion prospects, as well fiber size. The adhesion of the drug-loaded fiber to cellulose acetate membrane was compared to that of lamb esophageal mucosa and found to be 10-fold higher in magnitude. However, changes in the strength of adhesion due to varying CMC concentrations resulted in trends that correlated well with each other, implying the possibility of replacing mucosa with artificial membranes in the studies emphasizing the trend variations rather than absolute quantity of mucoadhesion. A hypothesis of a possible relationship between mucoadhesion and interfacial geometry of adhering surface, deduced from classical mucoadhesion theories, was tested by comparing the AFM-derived roughness dimensions to the detaching forces (determined using a texture analyzer) in comparable fiber−mucosa models. A similar test between CMC content in the fibers and interfacial roughness was also conducted. Statistically significant (at $p < 0.05$ level) monotonic relationships between detaching forces and R_a, R_{max}, and CMC concentration were established, thus confirming a valid relationship between interfacial roughness following polymer−mucin interactions and magnitude of mucoadhesion. These relationships can therefore be explored further for alternative methods of quantifying mucoadhesion in similar models.

■ AUTHOR INFORMATION

Corresponding Author
*E-mail: m.edirisinghe@ucl.ac.uk.
ORCID ⬡
Duncan Q. M. Craig: 0000-0003-1294-8993
Mohan Edirisinghe: 0000-0001-8258-7914
Present Address
‖King's College London, Faculty of Life Sciences and Medicine, Institute of Pharmaceutical Science, Drug Delivery Group, Franklin-Wilkins Building, 150 Stamford Street, London SE1 9NH, U.K. (B.R.-A.).
Notes
The authors declare no competing financial interest.

■ REFERENCES

(1) Smart, J. D. The Basics and Underlying Mechanisms of Mucoadhesion. *Adv. Drug Delivery Rev.* **2005**, *57*, 1556−1568.
(2) Andrews, G. P.; Laverty, T. P.; Jones, D. S. Mucoadhesive Polymeric Platforms for Controlled Drug Delivery. *Eur. J. Pharm. Biopharm.* **2009**, *71*, 505−518.
(3) Mansuri, S.; Kesharwani, P.; Jain, K.; Tekade, R. K.; Jain, N. K. Mucoadhesion: A Promising Approach in Drug Delivery System. *React. Funct. Polym.* **2016**, *100*, 151−172.
(4) Malik, R.; Garg, T.; Goyal, A. K.; Rath, G. Polymeric Nanofibers: Targeted Gastro-Retentive Drug Delivery Systems. *J. Drug Targeting* **2015**, *23*, 109−124.
(5) Singh, H.; Sharma, R.; Joshi, M.; Garg, T.; Goyal, A. K.; Rath, G. Transmucosal Delivery of Docetaxel by Mucoadhesive Polymeric Nanofibers. *Artif. Cells, Nanomed., Biotechnol.* **2015**, *43*, 263−269.
(6) Carvalho, F. C.; Bruschi, M. L.; Evangelista, R. C.; Gremião, M. P. D. Mucoadhesive Drug Delivery Systems. *Braz. J. Pharm. Sci.* **2010**, *46*, 1−17.
(7) Huang, Y.; Leobandung, W.; Foss, A.; Peppas, N. A. Molecular Aspects of Muco-And Bioadhesion: Tethered Structures and Site-Specific Surfaces. *J. Controlled Release* **2000**, *65*, 63−71.
(8) Hägerström, H.; Edsman, K. Limitations of the Rheological Mucoadhesion Method: The Effect of the Choice of Conditions and the Rheological Synergism Parameter. *Eur. J. Pharm. Sci.* **2003**, *18*, 349−357.
(9) Kaelble, D. H.; Moacanin, J. A Surface Energy Analysis of Bioadhesion. *Polymer* **1977**, *18*, 475−482.
(10) Peppas, N. A.; Buri, P. A. Surface, Interfacial and Molecular Aspects of Polymer Bioadhesion on Soft Tissues. *J. Controlled Release* **1985**, *2*, 257−275.
(11) Leung, S.-H. S.; Robinson, J. R. Polymer Structure Features Contributing to Mucoadhesion. II. *J. Controlled Release* **1990**, *12*, 187−194.
(12) Chickering, D.; Mathiowitz, E. Bioadhesive Microspheres: I. A Novel Electrobalance-Based Method to Study Adhesive Interactions between Individual Microspheres and Intestinal Mucosa. *J. Controlled Release* **1995**, *34*, 251−262.
(13) Mathiowitz, E.; Chickering, D. E., III; Lehr, C.-M. *Bioadhesive Drug Delivery Systems: Fundamentals, Novel Approaches, and Development*; CRC Press: Boca Raton, 1999.
(14) Peppas, N. A.; Sahlin, J. J. Hydrogels as Mucoadhesive and Bioadhesive Materials: A Review. *Biomaterials* **1996**, *17*, 1553−1561.
(15) Mortazavi, S. A.; Smart, J. D. An Investigation of Some Factors Influencing the In Vitro Assessment of Mucoadhesion. *Int. J. Pharm.* **1995**, *116*, 223−230.
(16) Cook, M. T.; Khutoryanskiy, V. V. Mucoadhesion and Mucosa-Mimetic Materials—A Mini-Review. *Int. J. Pharm.* **2015**, *495*, 991−998.
(17) Rençber, S.; Karavana, S. Y.; Yılmaz, F. F.; Eraç, B.; Nenni, M.; Özbal, S.; Pekçetin, Ç.; Gurer-Orhan, H.; Hoşgör-Limoncu, M.; Güneri, P.; Ertan, G. Development, Characterization, and In Vivo Assessment of Mucoadhesive Nanoparticles Containing Fluconazole for The Local Treatment of Oral Candidiasis. *Int. J. Nanomed.* **2016**, *11*, 2641−2653.
(18) Joergensen, L.; Klösgen, B.; Simonsen, A. C.; Borch, J.; Hagesaether, E. New Insights into the Mucoadhesion of Pectins by AFM Roughness Parameters in Combination with SPR. *Int. J. Pharm.* **2011**, *411*, 162−168.
(19) Davidovich-Pinhas, M.; Bianco-Peled, H. Mucoadhesion: A Review of Characterization Techniques. *Expert Opin. Drug Delivery* **2010**, *7*, 259−271.
(20) Brako, F.; Raimi-Abraham, B.; Mahalingam, S.; Craig, D. Q.; Edirisinghe, M. Making Nanofibres of Mucoadhesive Polymer Blends for Vaginal Therapies. *Eur. Polym. J.* **2015**, *70*, 186−196.
(21) Illangakoon, U. E.; Mahalingam, S.; Colombo, P.; Edirisinghe, M. Tailoring the Surface of Polymeric Nanofibres Generated by Pressurised Gyration. *Surf. Innovations* **2016**, *4*, 167−178.

(22) Mahalingam, S.; Edirisinghe, M. Forming of Polymer Nanofibers by a Pressurised Gyration Process. *Macromol. Rapid Commun.* **2013**, *34*, 1134−1139.

(23) Raimi-Abraham, B. T.; Mahalingam, S.; Davies, P. J.; Edirisinghe, M.; Craig, D. Q. Development and Characterization of Amorphous Nanofiber Drug Dispersions Prepared using Pressurised Gyration. *Mol. Pharmaceutics* **2015**, *12*, 3851−3861.

(24) Xu, Z.; Mahalingam, S.; Basnett, P.; Raimi-Abraham, B.; Roy, I.; Craig, D.; Edirisinghe, M. Making Nonwoven Fibrous Poly (E-Caprolactone) Constructs for Antimicrobial and Tissue Engineering Applications by Pressurized Melt Gyration. *Macromol. Mater. Eng.* **2016**, *301*, 922−934.

(25) Davies, R.; Taylor, G. In *The Mechanics of Large Bubbles Rising Through Extended Liquids and Through Liquids In Tubes*, Proceedings of The Royal Society of London A: Mathematical, Physical And Engineering Sciences; The Royal Society, 1950; Vol. *200*, pp 375−390.

(26) Brako, F.; Raimi-Abraham, B. T.; Mahalingam, S.; Craig, D. Q.; Edirisinghe, M. The Development of Progesterone-Loaded Nanofibers using Pressurized Gyration: A Novel Approach to Vaginal Delivery for the Prevention of Pre-Term Birth. *Int. J. Pharm.* **2018**, 31−39.

(27) Owen, D. H.; Katz, D. F. A Vaginal Fluid Simulant. *Contraception* **1999**, *59*, 91−95.

(28) Prasanna, R. I.; Anitha, P.; Chetty, C. M. Formulation and Evaluation of Bucco-Adhesive Tablets of Sumatriptan Succinate. *Int. J. Pharm. Invest.* **2011**, *1*, 182−191.

(29) Khdair, A.; Hamad, I.; Al-Hussaini, M.; Albayati, D.; Alkhatib, H.; Alkhalidi, B. In Vitro Artificial Membrane-Natural Mucosa Correlation of Carvedilol Buccal Delivery. *J. Drug Delivery Sci. Technol.* **2013**, *23*, 603−609.

(30) Pendergrass, P. B.; Belovicz, M. W.; Reeves, C. A. Surface Area of The Human Vagina as Measured from Vinyl Polysiloxane Casts. *Gynecol. Obstet. Invest.* **2003**, *55*, 110−113.

(31) Khutoryanskiy, V. V. Advances in Mucoadhesion and Mucoadhesive Polymers. *Macromol. Biosci.* **2011**, *11*, 748−764.

(32) Poller, B.; Strachan, C.; Broadbent, R.; Walker, G. F. A Minitablet Formulation Made from Electrospun Nanofibers. *Eur. J. Pharm. Biopharm.* **2017**, *114*, 213−220.

(33) Ball, C.; Woodrow, K. A. Electrospun Solid Dispersions of Maraviroc for Rapid Intravaginal Preexposure Prophylaxis of HIV. *Antimicrob. Agents Chemother.* **2014**, *58*, 4855−4865.

(34) Salalha, W.; Dror, Y.; Khalfin, R. L.; Cohen, Y.; Yarin, A. L.; Zussman, E. Single-Walled Carbon Nanotubes Embedded in Oriented Polymeric Nanofibers by Electrospinning. *Langmuir* **2004**, *20*, 9852−9855.

(35) Nam, S. H.; Shim, H.-S.; Kim, Y.-S.; Dar, M. A.; Kim, J. G.; Kim, W. B. Ag or Au Nanoparticle-Embedded One-Dimensional Composite Tio2 Nanofibers Prepared via Electrospinning for use In Lithium-Ion Batteries. *ACS Appl. Mater. Interfaces* **2010**, *2*, 2046−2052.

(36) Llorens, E.; Del Valle, L. J.; Díaz, A.; Casas, M. T.; Puiggalí, J. Polylactide Nanofibers Loaded with Vitamin B6 and Polyphenols as Bioactive Platform for Tissue Engineering. *Macromol. Res.* **2013**, *21*, 775−787.

(37) Padron, S.; Fuentes, A.; Caruntu, D.; Lozano, K. Experimental Study of Nanofiber Production through Forcespinning. *J. Appl. Phys.* **2013**, *113*, No. 024318.

(38) Yang, X. H.; Zhu, W. L. Viscosity Properties of Sodium Carboxymethylcellulose Solutions. *Cellulose* **2007**, *14*, 409−417.

(39) Barba, C.; Montané, D.; Farriol, X.; Desbrières, J.; Rinaudo, M. Synthesis and Characterization of Carboxymethylcelluloses from Non-Wood Pulps II. Rheological Behavior of CMC in Aqueous Solution. *Cellulose* **2002**, *9*, 327−335.

(40) Ivarsson, D.; Wahlgren, M. Comparison Of In Vitro Methods of Measuring Mucoadhesion: Ellipsometry, Tensile Strength and Rheological Measurements. *Colloids Surf., B* **2012**, *92*, 353−359.

(41) Boegh, M.; Foged, C.; Müllertz, A.; Nielsen, H. M. Mucosal Drug Delivery: Barriers, In Vitro Models and Formulation Strategies. *J. Drug Delivery Sci. Technol.* **2013**, *23*, 383−391.

(42) Jain, A. C.; Aungst, B. J.; Adeyeye, M. C. Development and In Vivo Evaluation of Buccal Tablets Prepared using Danazol−

Sulfobutylether 7 B-Cyclodextrin (SBE 7) Complexes. *J. Pharm. Sci.* **2002**, *91*, 1659−1668.

(43) Patel, M. M.; Smart, J. D.; Nevell, T. G.; Ewen, R. J.; Eaton, P. J.; Tsibouklis, J. Mucin/Poly (Acrylic Acid) Interactions: A Spectroscopic Investigation of Mucoadhesion. *Biomacromolecules* **2003**, *4*, 1184−1190.

(44) Park, H.; Robinson, J. R. Mechanisms of Mucoadhesion of Poly (Acrylic Acid) Hydrogels. *Pharm. Res.* **1987**, *4*, 457−464.

(45) Gardner, D. J.; Oporto, G. S.; Mills, R.; Samir, M. A. S. A. Adhesion and Surface Issues In Cellulose and Nanocellulose. *J. Adhes. Sci. Technol.* **2008**, *22*, 545−567.

(46) Tamayo, J.; Garcia, R. Deformation, Contact Time, and Phase Contrast in Tapping Mode Scanning Force Microscopy. *Langmuir* **1996**, *12*, 4430−4435.

(47) Stark, M.; Möller, C.; Müller, D. J.; Guckenberger, R. From Images to Interactions: High-Resolution Phase Imaging in Tapping-Mode Atomic Force Microscopy. *Biophys. J.* **2001**, *80*, 3009−3018.